American Mineralogist, Volume 94, pages 1440–1449, 2009

Sursassite: Hydrogen bonding, cation order, and pumpellyite intergrowth

Mariko Nagashima,[1,]* Masahide Akasaka,[2] Tetsuo Minakawa,[3] Eugen Libowitzky,[4] and Thomas Armbruster[1]

[1]Mineralogical Crystallography, Institute of Geological Sciences, University of Bern, Freiestrasse 3, CH-3012 Bern, Switzerland
[2]Department of Geoscience, Faculty of Science and Engineering, Shimane University, Matsue 690-8504, Japan
[3]Department of Earth Science, Faculty of Science, Ehime University, Matsuyama 790-5877, Japan
[4]Institute of Mineralogy and Crystallography, University of Vienna—Geocenter, Althanstrasse 14, A-1090 Vienna, Austria

Abstract

The crystal chemistry of sursassite, simplified formula $Mn_2^{2+}Al_3Si_3O_{11}(OH)_3$, from six different localities [(1) Falotta, Switzerland, (2) Woodstock, New Brunswick, Canada, (3) Kamisugai, Japan, (4) Kamogawa, Japan, (5) Molinello, Italy, and (6) Gambatesa, Italy] was studied using electron microprobe analysis (EMPA), Fourier transform infrared spectroscopy (FTIR), and single-crystal X-ray diffraction methods. The structure has two symmetry independent Mn sites. The Mn1 site is seven coordinated by O and hosts, in addition to Mn^{2+}, up to 20% Ca, whereas Mn2 has octahedral coordination and is strongly selective for Mn^{2+}. In the simplified formula, three smaller octahedral M sites are occupied by Al. However, M1 also accepts significant amounts of divalent cations, such as Cu, Mg, Fe, and Mn, whereas M2 is occupied exclusively by Al. The unit-cell parameters of sursassite are a = 8.698–8.728, b = 5.789–5.807, c = 9.778–9.812 Å, β = 108.879–109.060°, V = 465.7–470.0 Å^3, the space group is $P2_1/m$. Structure refinements converged to R_1 values of 2.15–6.62%. In agreement with bond-valence analyses, at least three OH groups, depending on the concentration of divalent cations at M1, are found at the O6, O7, and O11 positions. However, the bond-valence sum at O10 is always low, thus partial hydroxylation is assumed at O10 to maintain charge balance. Owing to the influence of divalent cations at M1 in sursassite the hydrogen-bond systems in sursassite and isostructural macfallite are different. The FTIR spectrum in the region of OH-stretching vibrations is characterized by three strong bands at 3511, 3262, and around 2950 cm^{-1}, the latter being broad. The band at 2950 cm^{-1} is assigned to strong hydrogen bonds between O6 and O10 (O6···O10 = 2.66 Å). Residual difference-Fourier peaks in the refinement of the Kamogawa and Molinello (specimen 1) crystals indicated less than 5% pumpellyite intergrowth.

Keywords: Sursassite, hydrogen bond, infrared spectroscopy, crystal structure, macfallite, pumpellyite

Introduction

Silicate minerals stable at low temperatures are commonly hydrous and complex both structurally and chemically. Owing to the small size of crystals and compositional heterogeneity, the crystal structure and phase transitions of these minerals have not been adequately studied. One of these hydrous silicates is sursassite, with the simplified formula $Mn_2^{2+}Al_3Si_3O_{11}(OH)_3$. It has been reported from several localities. The type locality of sursassite is Parsettens at Val d'Err, Graubünden, Switzerland (Jakob 1926, 1931, 1933). The simplified formula and space group $P2_1/m$ were determined by Freed (1964). The crystal structure of sursassite was first solved by Mellini et al. (1984) (R = 6.5%). The general formula is $[^{VII}Mn1^{VI}Mn2][^{VI}Al1^{VI}Al2^{VI}Al3][^{IV}SiO_4][^{IV}Si_2O_7](OH)_3$, indicating that orthosilicate and disilicate groups have a 1:1 ratio. Allmann (1984) also refined the crystal structure of sursassite (R = 6.6%) and determined site occupancies, but did not provide any details on the analytical procedure. Polysomatic descriptions of isostructural sursassite and macfallite, as well as of pumpellyite, ardennite, and lawsonite, all of which are the so-called 6 × 9 Å structures with corresponding axial translations, were presented by Moore et al. (1985) and Ferraris et al. (1986, 2004).

A systematic study of the structural and chemical relations in sursassite could not be done until recently because of the very thin and fibrous nature of most specimens of this mineral. Thus, such a study would require either synchrotron radiation or very sensitive X-ray area detectors, which are now available even for in-house laboratory X-ray equipment. The fibrous crystals measured in this study are commonly less than 0.1 mm in length and 0.02 mm in their shortest dimension.

In this study, we investigated the crystal chemistry of seven sursassite crystals from six different localities to examine the structural and compositional relationships between sursassite and macfallite, including the nature of their hydrogen bonding systems. The following experimental methods were used: elec-

* E-mail: mariko.nagashima@krist.unibe.ch

0003-004X/09/0010–1440$05.00/DOI: 10.2138/am.2009.3223

tron microprobe analysis (EMPA), Fourier transform infrared spectroscopy (FTIR), and single-crystal X-ray diffraction. A bond-valence analysis was also carried out.

EXPERIMENTAL METHODS

Samples

Seven sursassite samples from six different localities were used in this study, including: (1) sursassite-bearing quartz veinlets penetrating Mn ore in the Oberhalbstein Alps, at Falotta, Graubünden, Switzerland (Jakob 1933), a locality ca. 10 km west of Parsettens at Val d'Err (type locality); (2) barite-quartz-calcite veinlets with sursassite occurring in a Fe-Mn ore deposit near Woodstock, New Brunswick, Canada (Heinrich 1962; Freed 1964); (3) metamorphic manganese deposit at Kamisugai in the Sambagawa metamorphic belt, Ohzu, Ehime, Japan (Minakawa 1992); (4) metamorphic manganese deposit at Kamogawa in the Sambagawa metamorphic belt, Ehime, Japan (Minakawa and Momoi 1987); (5) two samples from the manganese mine at Molinello, Liguria, Italy (Cortesogno et al. 1979; Marchesini and Pagano 2001); and (6) the manganese mine at Gambatesa, Liguria, Italy (Cortesogno et al. 1979; Marchesini and Pagano 2001).

Sursassite occurs as fibrous crystals elongated parallel to the **b** axis and up to 2 mm long. The crystals form massive or radiating aggregates, are yellowish brown, and pleochroic from colorless to pale yellow in plane-polarized light.

Chemical analysis (EMPA)

The chemical composition of sursassite was determined using a JEOL JXA-8200 electron probe microanalyzer at the University of Bern. The abundances of Si, Ti, Al, Cr, V, Fe, Mn, Mg, Ca, Ba, Na, K, Cu, Zn, Pb, and Ni were measured using an accelerating voltage of 15 kV and a beam current of 20 nA, with a beam diameter of 1 μm. The following standards were used: natural wollastonite (Si, Ca), synthetic ilmenite (Ti), anorthite (Al), synthetic eskolaite (Cr), synthetic shcherbinaite (V), synthetic almandine (Fe), synthetic tephroite (Mn), synthetic spinel (Mg), natural barite (Ba), natural albite (Na), natural orthoclase (K), natural tennantite (Cu), synthetic gahnite (Zn), natural crocoite (Pb), and synthetic bunsenite (Ni). The PRZ method (modified ZAF) was used for data correction for all elements.

Semi-quantitative Mn^{2+}/Mn^{3+} ratios in sursassite were determined using the ratio of the X-ray intensities of the Mn$L\beta$ and Mn$L\alpha$ lines after the method of Albee and Chodos (1970) and Kimura and Akasaka (1999). For this purpose, the X-ray intensities were measured using a JEOL JXA-8800M electron-probe microanalyzer at Shimane University, Japan, using a TAP monochromator for a range of L values between 206 and 213 mm with a step interval of 0.05 mm and a step counting time of 10 s. The L values are the distances between the measuring spot on the sample and the point on the TAP crystal where the X-ray beam impinges, and are related to the wavelength of X-rays (λ in angstroms) by the equation $L = (R/d) \times n\lambda$, where R is the radius of the Rowland circle (R = 140 mm for the JEOL JXA-8800M), d the (001) interplanar spacing (Å) of the TAP crystal, and n the order of Bragg reflection. The measured spectra were fitted with Lorentzian curves by least-squares methods to determine peak positions, peak widths, and peak intensities using a program written by Kimura and Akasaka (1999). The equation, $I(\mathrm{Mn}L\beta)/I(\mathrm{Mn}L\alpha) = 0.46 \times Mn^{2+}/(Mn^{2+} + Mn^{3+}) + 0.554$ (Kimura and Akasaka 1999), where I represents peak intensity, was employed for the estimation of the Mn^{2+}/Mn^{3+} ratio.

Fourier-transform infrared (FTIR) spectroscopy

IR powder spectra were obtained on a BRUKER TENSOR 27 FTIR spectrometer at the University of Vienna. A global MIR light source, a 6 mm aperture, a KBr beam splitter, and a DLaTGS detector were used to collect spectra in the wavenumber range from 370 to 4000 cm^{-1}. Two different measurement techniques were applied. To avoid any interference from water impurities in KBr, spectra of undiluted sample powder were measured on a HARRICKMVP2 diamond attenuated-total-reflectance (ATR) accessory (technique 1). However, because ATR spectra show some red-shift of absorption bands, conventional KBr pellets were also prepared at different dilution ratios and measured in transmission mode in the conventional sample compartment (technique 2). Sample and background spectra were averaged from each of 32 scans at 4 cm^{-1} resolution. The reference spectra were acquired: (1) from the empty ATR unit in air, or (2) from a pure KBr pellet without the sample. Data handling was performed with the OPUS 5.5 software.

Single-crystal structure analysis

X-ray diffraction data for single crystals of sursassite were collected using a Bruker SMART APEX II CCD diffractometer of Bruker AXS K.K. Crystals were mounted on glass fibers and intensity data were measured at room temperature using graphite-monochromatized Mo$K\alpha$ radiation (λ = 0.71069 Å). Preliminary lattice parameters and an orientation matrix were obtained from three sets of frames and refined during the integration process of the intensity data. Diffraction data were collected with ω scans at different φ settings (φ-ω scan) (Bruker 1999). Data were processed using SAINT (Bruker 1999). An empirical absorption correction using SADABS (Sheldrick 1996) was applied, but TWINABS (Sheldrick 2002) was only used for the Gambatesa sursassite. The reflection statistics and systematic absences were consistent with space groups $P2_1$ and $P2_1/m$. Subsequent attempts to solve the structure indicated that the observed average structure is centrosymmetric and for this reason $P2_1/m$ is the correct space group. Structural refinement was performed using SHELXL-97 (Sheldrick 1997). Scattering factors for neutral atoms were employed. Positions of the H atoms of the hydroxyl groups were derived from difference-Fourier syntheses. Subsequently, H positions were refined at a fixed value of U_{iso} = 0.05 Å^2. For better direct comparison with isostructural macfallite (Nagashima et al. 2008), we use in this study the more general symbols M1, M2, and M3 to denote the three octahedrally coordinated sites normally populated with Al. The structural formula of sursassite is $[^{VII}Mn1^{VI}Mn2][^{VI}M1^{VI}M2^{VI}M3][^{IV}SiO_4][^{IV}Si_2O_7](OH)_3$. The site populations for Mn1, Mn2, M1, M2, and M3 were determined in accord with the procedure described by Hawthorne et al. (1995). The H positions were refined with a bond distance constraint of O-H = 0.98 Å (Franks 1973). The anisotropic displacement parameters for O2, O7, and O11 of sursassite from Molinello, Italy, did not converge to physically meaningful values. The poor data quality allowed for only isotropic displacement parameters for these oxygen sites to be refined.

RESULTS

Chemical compositions of sursassite

The average chemical compositions of the seven studied sursassite samples from six different localities are given in Table 1, where total Mn is reported as MnO. The total MnO concentration varies between 24.5–27.1 wt%. It is noteworthy that sursassite from the Molinello mine (specimen 2) is characterized by a high Cu concentration (1.4–2.4 wt% CuO). The corresponding crystal-chemical formulae are summarized in Table 1, where the total number of cations, except H ions, was normalized to 8 and the amount of OH was calculated to obtain electroneutrality. There are upper and lower limits to the number of O and OH, depending on whether Mn in the M1 and M3 sites is considered Mn^{2+} or Mn^{3+}. A semi-quantitative estimate of the Mn^{2+}/Mn^{3+} ratio in sursassite from Woodstock using the method of Kimura and Akasaka (1999) indicates that 46–52% of the Mn in this sample is divalent. Given the low accuracy of this method (±10%), most of Mn at the M1 and M3 sites in this sample might be trivalent. The presence of Mn^{2+} and Mn^{3+} has also been confirmed for the samples from Falotta and Kamisugai, but the high associated standard deviation did not allow a reliable estimate of the Mn^{2+}/Mn^{3+} ratio to be made for these samples. The sursassite crystals used for the X-ray single-crystal refinement were picked from hand specimens and analyzed by electron microprobe. Therefore, the average chemical composition for each sample in Table 1 was used to constrain Ca, Mg, Fe, and Cu contents in the site population refinements.

Infrared spectra

The ATR-FTIR spectrum of sursassite from Woodstock, New Brunswick, between 3800 and 2400 cm^{-1} is shown in Figure 1. Two absorption bands at 3511 and 3262 cm^{-1} and an additional broad absorption band at ca. 2950 cm^{-1} have been assigned to OH vibrations. The absorption spectrum of a KBr sample pellet confirmed the OH-stretching vibrations at slightly higher wavenumbers. A similar IR spectrum was also observed by Reddy and Frost (2007).

Table 1. Average chemical compositions of the sursassite samples (n, number of data)

Locality	Falotta, Switzerland		New Brunswick, Canada		Kamisugai, Japan		Kamogawa, Japan		Molinello, Italy (Specimen 1)		Molinello, Italy (Specimen 2)		Gambatesa, Italy	
Sample no.	1		2		3		4		5		6		7	
	n = 30		n = 35		n = 46		n = 30		n = 34		n = 24		n = 34	
	avg.	s.d.	avg.	s.d.	avg.	s.d.	avg.	s.d.	avg.	s.d.	avg.	s.d.	avg.	s.d.
SiO_2	35.79	0.23	34.87	0.94	34.62	1.20	34.55	0.28	34.98	0.57	34.97	0.52	35.49	0.58
TiO_2	0.04	0.04	0.03	0.03	0.09	0.07	0.06	0.03	0.05	0.03	0.05	0.03	0.05	0.03
Al_2O_3	22.99	0.79	24.49	1.02	21.00	1.35	24.28	0.57	25.10	0.81	24.60	1.08	25.56	0.39
Fe_2O_3*	0.17	0.22	0.08	0.24	0.60	0.59	0.78	0.11	0.01	0.05	0.02	0.07	–	
V_2O_3*	0.02	0.03	0.01	0.01	0.08	0.21	0.09	0.06	0.20	0.28	0.19	0.29	0.06	0.10
MnO*	25.61	0.71	26.77	1.13	28.45	2.21	25.21	0.87	25.02	1.44	24.29	1.32	22.80	1.90
MgO	2.61	0.11	2.27	0.23	2.36	0.28	1.75	0.46	2.02	0.23	1.45	0.21	2.22	0.20
CaO	4.28	0.37	2.35	0.32	3.14	0.89	3.62	0.52	3.69	0.92	4.18	0.86	5.14	1.44
CuO	0.05	0.07	0.05	0.07	0.06	0.08	0.11	0.07	0.53	0.26	1.89	0.30	0.05	0.08
ZnO	0.04	0.06	0.06	0.06	0.06	0.07	–	0.03	0.05	0.03	0.05		0.02	0.04
	91.60		90.98		90.46		90.45		91.63		91.67		91.39	
							Σ cations = 8							
Si	3.08	0.02	3.01	0.05	3.03	0.06	3.01	0.02	3.00	0.03	3.02	0.04	3.03	0.04
Ti	0.00	0.00	0.00	0.00	0.01	0.00	0.00	0.00	0.00	0.00	0.00	0.00	0.00	0.00
Al	2.33	0.07	2.50	0.08	2.17	0.14	2.49	0.06	2.54	0.07	2.50	0.09	2.57	0.05
Fe^{3+}	0.01	0.01	0.01	0.02	0.04	0.04	0.05	0.00	0.00	0.00	0.00	0.01	–	
V^{3+}	0.00	0.00	0.00	0.00	0.01	0.01	0.01	0.00	0.01	0.02	0.01	0.02	0.00	0.01
Mn^{2+}	1.86	0.05	1.96	0.10	2.12	0.16	1.86	0.06	1.82	0.11	1.77	0.10	1.65	0.13
Mg	0.33	0.01	0.29	0.03	0.31	0.04	0.23	0.06	0.26	0.03	0.19	0.03	0.28	0.02
Ca	0.39	0.04	0.22	0.03	0.30	0.08	0.34	0.05	0.34	0.09	0.39	0.08	0.47	0.13
Cu	0.00	0.00	0.00	0.00	0.00	0.01	0.01	0.01	0.03	0.02	0.12	0.02	0.00	0.00
Zn	0.00	0.01	0.01	0.01	0.01	0.01	–		0.00	0.00	0.00	0.01	0.00	0.00

* Total Fe as Fe_2O_3, V as V_2O_3, and Mn as MnO.

1: $(Mn^{2+}_{1.61}Ca_{0.39})_{\Sigma 2.00}(Mn_{0.25}Al_{2.33}Mg_{0.33}Fe^{3+}_{0.01})_{\Sigma 2.92}Si_{3.08}O_{10.49–10.74}(OH)_{3.26–3.51}$.

2: $(Mn^{2+}_{1.78}Ca_{0.22})_{\Sigma 2.00}(Mn_{0.18}Al_{2.50}Mg_{0.29}Fe^{3+}_{0.01}Zn_{0.01})_{\Sigma 2.99}Si_{3.01}O_{10.53–10.71}(OH)_{3.29–3.47}$.

3: $(Mn^{2+}_{1.70}Ca_{0.30})_{\Sigma 2.00}(Mn_{0.42}Al_{2.17}Mg_{0.31}Fe^{3+}_{0.04}V^{3+}_{0.01}Ti_{0.01}Zn_{0.01})_{\Sigma 2.97}Si_{3.03}O_{10.31–10.73}(OH)_{3.27–3.69}$.

4: $(Mn^{2+}_{1.66}Ca_{0.34})_{\Sigma 2.00}(Mn_{0.20}Al_{2.49}Mg_{0.23}Fe^{3+}_{0.05}V^{3+}_{0.01}Cu_{0.01})_{\Sigma 2.99}Si_{3.01}O_{10.57–10.77}(OH)_{3.23–3.43}$.

5: $(Mn^{2+}_{1.66}Ca_{0.34})_{\Sigma 2.00}(Mn_{0.16}Al_{2.54}Mg_{0.26}V^{3+}_{0.01}Cu_{0.03})_{\Sigma 3.00}Si_{3.00}O_{10.51–10.71}(OH)_{3.29–3.45}$.

6: $(Mn^{2+}_{1.61}Ca_{0.39})_{\Sigma 2.00}(Mn_{0.16}Al_{2.50}Mg_{0.19}V^{3+}_{0.01}Cu_{0.12})_{\Sigma 2.98}Si_{3.02}O_{10.55–10.81}(OH)_{3.29–3.45}$.

7: $(Mn^{2+}_{1.53}Ca_{0.57})_{\Sigma 2.00}(Mn_{0.12}Al_{2.57}Mg_{0.28})_{\Sigma 2.97}Si_{3.03}O_{10.63–10.75}(OH)_{3.25–3.37}$.

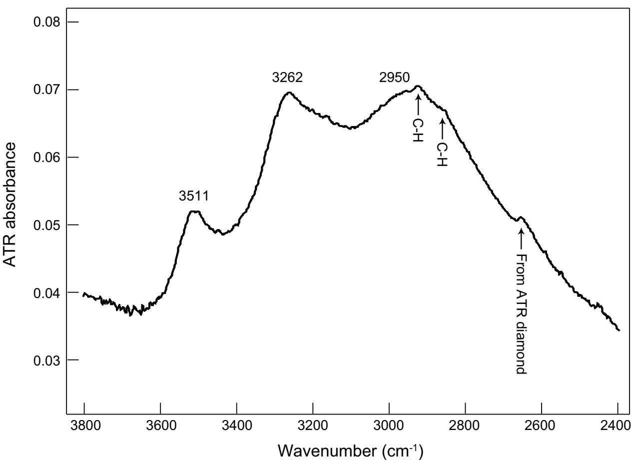

Figure 1. ATR-FTIR spectrum of sursassite between 3800–2400 $cm^{–1}$.

Crystal structure solution and refinements

Crystallographic data and refinement parameters are summarized in Table 2. The refined atomic positions and anisotropic displacement parameters are listed in Tables 3[1] and 4[1]. Interatomic distances and angles for hydrogen bonds are presented in Table 5. Table 6 gives the site-scattering values and cation assignments. The crystal structure of sursassite is shown in Figure 2.

According to the measured site-scattering values, Ca favors the Mn1 site over Mn2 (Table 6). This is consistent with the polyhedral volumes: $Mn1O_7 > Mn2O_6$. Moreover, site-scattering values and M2-O distances indicate that the M2 site is occupied by Al only. The Al and Mn site populations at the M1 and M3 sites were calculated by the following procedure: (1) elements with less than 0.01 atoms per formula unit (apfu) were omitted; (2) Mg^{2+} and Cu^{2+} were assigned to the M1 site because the volume of the $M1O_6$ octahedron is the largest among the three independent MO_6 octahedra; and (3) the following constraints were applied: $g(Al) + g(Mn) = 1 – g(Mg) – g(Cu)$ for the M1 site and $g(Al) + g(Mn) = 1$ for the M3 site, where g represents site population (apfu). The resulting cation populations are given in Table 6.

Bond-valence sums were calculated using the electrostatic strength function of Brown and Altermatt (1985) and the bond-valence parameters of Brese and O'Keeffe (1991). The results are given in Table 7. Manganese was calculated as divalent at Mn1 and Mn2 and as trivalent at M1, M2, and M3. The calculated bond-valence sums and refined hydrogen positions indicate that hydroxyl groups are located at O6, O7, and O11. Although no hydrogen position could be found close to O10, the bond-valence sum for this position (Table 7) suggests that O10 not only acts as an acceptor but also as a donor of a hydrogen bond.

[1] Deposit item AM-09-046, Tables 3 and 4 (refined atomic positions and anisotropic displacement parameters). Deposit items are available two ways: For a paper copy contact the Business Office of the Mineralogical Society of America (see inside front cover of recent issue) for price information. For an electronic copy visit the MSA web site at http://www.minsocam.org, go to the American Mineralogist Contents, find the table of contents for the specific volume/issue wanted, and then click on the deposit link there.

TABLE 2. Experimental details of the single-crystal X-ray diffraction analyses of sursassite

Sample locality	Falotta, Switzerland	New Brunswick, Canada	Kamisugai, Japan	Kamogawa, Japan	Molinello, Italy (Specimen 1)	Molinello, Italy (Specimen 2)	Gambatesa, Italy
Sample no.	1	2	3	4	5	6	7
Crystal size (mm)	0.06 × 0.05 × 0.025	0.09 × 0.08 × 0.01	0.014 × 0.01 × 0.01	0.135 × 0.07 × 0.02	0.045 × 0.04 × 0.025	0.09 × 0.045 × 0.015	0.08 × 0.03 × 0.015
Cell parameters							
a (Å)	8.7201(1)	8.709(1)	8.7278(4)	8.7065(2)	8.6982(2)	8.716(4)	8.715(1)
b (Å)	5.8053(1)	5.7939(7)	5.8065(2)	5.7978(1)	5.7887(1)	5.799(3)	5.7981(8)
c (Å)	9.8075(1)	9.779(1)	9.8121(3)	9.7946(3)	9.7777(2)	9.794(5)	9.798(1)
β (°)	109.011(1)	108.953(6)	109.060(3)	108.938(2)	108.918(1)	108.985(5)	108.879(4)
V ($Å^3$)	469.40(2)	466.68(10)	470.00(5)	467.65(3)	465.73(2)	468.09(9)	468.43(7)
D_{calc} (g/cm^3)	3.561	3.588	3.609	3.575	3.584	3.586	3.532
θ_{min} (°)	2.2	2.7	4.7	2.7	2.2	2.2	2.2
θ_{max} (°)	30.5	30.0	30.4	30.5	30.0	24.1	30.0
Absorption coefficient μ (mm^{-1})	3.42	3.48	3.45	4.02	4.04	3.47	3.47
Collected reflections	10136	4493	4392	4689	7134	1564	5994
Unique reflections	1562	1455	1540	1539	1486	760	2682
R_{int} (%)	2.49	4.82	5.07	2.21	3.22	5.32	twin
Index limits	$-12\leq h\leq 12, -8\leq k\leq 8, -13\leq l\leq 14$	$-9\leq h\leq 12, -8\leq k\leq 7, -13\leq l\leq 13$	$-11\leq h\leq 12, -8\leq k\leq 8, -13\leq l\leq 13$	$-12\leq h\leq 12, -7\leq k\leq 8, -12\leq l\leq 13$	$-11\leq h\leq 12, -5\leq k\leq 8, -13\leq l\leq 11$	$-9\leq h\leq 9, -6\leq k\leq 5, -10\leq l\leq 11$	$-12\leq h\leq 11, 0\leq k\leq 8, 0\leq l\leq 13$
GooF	1.115	1.017	0.990	1.087	1.084	1.017	1.049
R_1 (%)	2.15	4.48	4.38	3.53	3.51	4.99	6.62
wR_2 (%)	5.83	11.90	10.53	9.69	9.31	12.39	18.56
No. of parameters	139	135	129	139	139	118	134
Weighting scheme	$\omega = 1/[\sigma^2(F_o^2) + (0.0301P)^2 + 0.40P]$	$\omega = 1/[\sigma^2(F_o^2) + (0.0629P)^2 + 0.59P]$	$\omega = 1/[\sigma^2(F_o^2) + (0.0509P)^2]$	$\omega = 1/[\sigma^2(F_o^2) + (0.0540P)^2] + 0.69P$	$\omega = 1/[\sigma^2(F_o^2) + (0.0502P)^2 + 0.7P]$	$\omega = 1/[\sigma^2(F_o^2) + (0.0597P)^2 + 1.47P]$	$\omega = 1/[\sigma^2(F_o^2) + (0.0938P)^2 + 1.69P]$
$\Delta\rho_{max}$ ($e/Å^3$)	0.555	0.837	0.950	2.307	2.083	0.773	2.072
$\Delta\rho_{min}$ ($e/Å^3$)	−0.456	−0.905	−0.811	−0.824	−1.000	−0.815	−1.604

Note: X-ray diffraction data were collected using a Bruker SMART APEX II CCD diffractometer. Intensity data were measured at room temperature using graphite-monochromatized Mo*K*α radiation (λ = 0.71069 Å). Diffraction data were collected with φ-ω scan (Bruker 1999). Data were processed using SAINT (Bruker 1999). An empirical absorption correction using SADABS (Sheldrick 1996) for Falotta, New Brunswick, Kamisugai, Kamogawa, and Molinello samples, and TWINABS (Sheldrick 2002) for the Gambatesa sample was applied. The space group of sursassite was $P2_1/m$. Structural refinement was performed using SHELXL-97 (Sheldrick 1997). The function of the weighting scheme is $\omega = 1/[\sigma^2(F_o^2) + (a\cdot P)^2 + b\cdot P]$, where $P = [Max(F_o^2, 0) + 2F_c^2]/3$, and the parameters *a* and *b* are chosen to minimize the diffrerences in the variances for reflections in different ranges of intensity and diffraction angle.

DISCUSSION

Cation distributions at the octahedral sites in sursassite, macfallite, and pumpellyite

Allmann (1984) determined the site occupancies in sursassite from Andros (Greece) as 0.8Mn + 0.2Ca for Mn1, 0.85Mn + 0.15Ca for Mn2, 0.31Al + 0.39Mg + 0.30Mn for M1, 1.00Al for M2, and 0.85Al + 0.12Fe + 0.03Mn for M3. In addition, Mellini et al. (1984) refined the crystal structure of sursassite from Monte Alpe, Italy, but obvious pumpellyite intergrowth hampered meaningful cation assignment. Results of this study are similar to those of Allmann (1984). According to the site-scattering values determined in this study, Ca has a strong preference for Mn1 over Mn2. The exact oxidation state of manganese at M1 and M3 is unknown, but bond distances, bond-length distortions, and semi-quantitative analysis of Mn^{2+}/Mn^{3+} ratios strongly suggest that in the M sites, Mn occurs as Mn^{3+} rather than as Mn^{2+}.

The crystal structures of sursassite [$Mn_2^{2+}Al_3Si_3O_{11}(OH)_3$], macfallite [$Ca_2Mn_3^{3+}Si_3O_{11}(OH)_3$], and pumpellyite [$Z = 1$, space group $A2/m$, $Ca_8X_4^{VI}Y_8^{VI}Si_{12}O_{56-n}(OH)_n$] are closely related to each other (Allmann 1984; Mellini et al. 1984; Moore et al. 1985; Ferraris et al. 1986). Subordinate divalent cations are located at M1 in sursassite and macfallite (Nagashima et al. 2008) as well as at X in pumpellyite. $M1O_6$-octahedra in sursassite and macfallite and XO_6-octahedra in pumpellyite are topologically similar to one another. The chemical compositions determined in this study indicate that sursassite always contains some divalent cations replacing octahedral Al, which confirms the conclusions reached in the previous studies (e.g., Heinrich 1962; Allmann 1984; Mellini et al. 1984; Reinecke 1986; Minakawa and Momoi 1987; Hatert et al. 2008). Although the ratio of M^{2+} to M^{3+} at X in pumpellyite is almost 1:1, M1 in sursassite is occupied by 0.25–0.3 M^{2+} + 0.7–0.75 M^{3+} (if all Mn at M1 is assumed trivalent). Thus, it is concluded that small amounts of divalent cations are necessary for the formation of sursassite, as well as pumpellyite, but the amount of M^{2+} at M1 in sursassite is less than that at X in pumpellyite. Additional evidence is the composition of the synthetic high-pressure phase $Mg_4(MgAl)Al_4[Si_6O_{21}/(OH)_7]$, a structural analogue of sursassite (Gottschalk et al. 2000).

Structural variation due to cation substitution

The variation of the unit-cell parameters as a function of Ca^{Mn1} + $(Mg + Cu + Mn)^{M1+M3}$ (apfu) is shown in Figure 3 and display positive correlations. On the other hand, the influence of the Ca ↔ Mn^{2+} substitution at Mn1 is not seen in a systematic variation of cell dimensions.

Figure 4 shows the variation of M1-Oi distances with the mean ionic radius of the M1 cation. The mean M1-O distance increases with increasing mean ionic radius at M1 ($R^2 = 0.80$). Although the M1-O1 and M1-O5 distances also increase with increasing mean ionic radius, the increase of M1-O1 is considerably steeper. On the other hand, the M1-O7 distance is almost independent of the cation content. This nonuniform behavior is responsible for anisotropic expansion of $M1O_6$-octahedra with increasing ionic radius in M1.

Table 8 lists bond-length and angular distortion parameters defined by Baur (1974) and Robinson et al. (1971). The bond-length distortion of $M1O_6$-octahedra increases with Mn content at M1 ($R^2 = 0.80$) because of the O1-M1-O1 elongation (Fig. 5). This is probably due to Mn^{3+} Jahn-Teller distortion, supporting

TABLE 5. Selected interatomic distances (Å) and bond angles (°)

Sample		Falotta, Switzerland	New Brunswick, Canada	Kamisugai, Japan	Kamogawa, Japan	Molinello, Italy		Gambatesa, Italy
						(Specimen 1)	(Specimen 2)	
Mn1-O1	×2	2.328(1)	2.316(3)	2.317(3)	2.327(2)	2.334(2)	2.328(6)	2.334(4)
-O2	×2	2.225(1)	2.212(3)	2.223(3)	2.223(2)	2.217(2)	2.212(6)	2.227(4)
-O7		2.229(2)	2.212(4)	2.212(4)	2.227(3)	2.246(3)	2.218(9)	2.250(6)
-O8		2.393(2)	2.397(4)	2.411(4)	2.404(3)	2.391(3)	2.410(9)	2.398(5)
-O9		2.465(2)	2.462(4)	2.465(4)	2.455(3)	2.451(3)	2.465(8)	2.458(5)
avg.		2.313	2.304	2.310	2.312	2.313	2.310	2.318
Mn2-O1	×2	2.271(1)	2.265(3)	2.261(3)	2.267(2)	2.273(2)	2.269(6)	2.273(4)
-O3	×2	2.141(1)	2.137(3)	2.145(3)	2.140(2)	2.137(2)	2.148(7)	2.148(3)
-O5		2.529(2)	2.530(4)	2.485(4)	2.529(3)	2.584(3)	2.542(9)	2.589(5)
-O10		2.201(2)	2.189(4)	2.214(4)	2.198(3)	2.176(3)	2.213(9)	2.195(6)
avg.		2.259	2.254	2.252	2.257	2.263	2.265	2.271
M1-O1	×2	2.091(1)	2.093(3)	2.128(3)	2.090(2)	2.051(2)	2.084(6)	2.069(4)
-O5	×2	2.000(1)	1.997(3)	2.016(2)	1.995(2)	1.978(2)	2.001(6)	1.988(3)
-O7	×2	1.897(1)	1.893(3)	1.902(2)	1.898(2)	1.890(2)	1.892(6)	1.901(3)
avg.		1.996	1.994	2.015	1.994	1.973	1.992	1.986
M2-O3	×2	1.892(1)	1.891(3)	1.892(3)	1.887(2)	1.884(2)	1.900(5)	1.882(3)
-O4	×2	1.917(1)	1.914(2)	1.915(2)	1.916(2)	1.915(2)	1.917(5)	1.918(3)
-O11	×2	1.883(1)	1.883(2)	1.879(2)	1.879(2)	1.882(2)	1.880(5)	1.881(3)
avg.		1.897	1.896	1.895	1.894	1.894	1.899	1.894
M3-O2	×2	1.905(1)	1.897(3)	1.900(3)	1.898(2)	1.905(2)	1.907(5)	1.905(3)
-O6	×2	1.862(1)	1.858(2)	1.865(2)	1.858(2)	1.856(2)	1.864(5)	1.860(3)
-O8	×2	2.009(1)	1.997(3)	2.007(3)	1.997(2)	1.994(2)	2.005(6)	2.002(4)
avg.		1.925	1.917	1.924	1.918	1.918	1.925	1.922
Si1-O2	×2	1.622(1)	1.621(3)	1.619(3)	1.620(2)	1.622(2)	1.619(7)	1.622(4)
-O4		1.640(2)	1.644(4)	1.647(4)	1.641(3)	1.640(3)	1.646(9)	1.645(5)
-O5		1.653(2)	1.646(5)	1.643(4)	1.654(3)	1.655(3)	1.639(9)	1.646(5)
avg.		1.634	1.633	1.632	1.634	1.635	1.631	1.634
Si2-O3	×2	1.614(1)	1.613(3)	1.611(3)	1.613(2)	1.611(2)	1.596(7)	1.612(4)
-O8		1.652(2)	1.660(4)	1.658(4)	1.653(3)	1.654(3)	1.644(9)	1.650(5)
-O9		1.657(2)	1.645(4)	1.653(4)	1.654(3)	1.653(3)	1.643(9)	1.643(5)
avg.		1.634	1.633	1.633	1.633	1.632	1.620	1.629
Si3-O1	×2	1.639(1)	1.642(3)	1.637(3)	1.638(2)	1.645(2)	1.647(7)	1.647(4)
-O9		1.661(2)	1.667(4)	1.663(4)	1.665(3)	1.664(3)	1.671(9)	1.669(5)
-O10		1.625(2)	1.622(5)	1.632(4)	1.625(3)	1.614(3)	1.608(9)	1.619(6)
avg.		1.641	1.643	1.642	1.642	1.642	1.643	1.646
O6···O10		2.667(2)	2.658(6)	2.661(5)	2.669(4)	2.663(4)	2.66(1)	2.664(7)
O6···O3		2.925(2)	2.916(4)	2.935(4)	2.918(2)	2.907(2)	2.922(8)	2.912(5)
O6···O11		2.736(2)	2.737(5)	2.732(5)	2.739(3)	2.743(3)	2.743(9)	2.752(5)
O7···O11		2.853(2)	2.833(5)	2.862(5)	2.840(4)	2.823(4)	2.85(1)	2.824(6)
O7···O2		2.900(1)	2.895(3)	2.902(3)	2.901(2)	2.894(2)	2.899(7)	2.902(4)
O11···O2		2.855(2)	2.851(4)	2.868(4)	2.856(2)	2.844(2)	2.864(8)	2.855(5)
O6-H6A···O10		178(2)	177(2)		180(2)	178(2)		
O6-H6B···O3		118(1)			124(2)	122(2)		
O6-H6B···O11		155(1)			142(2)	145(2)		
O7-H7···O2						128(1)		
O7-H7···O11		162(1)	172(2)		175(2)			165(3)
O11-H11A···O2		117(1)	109(1)		122(2)	117(2)		
O11-H11A···O6		152(1)	168(1)		144(2)	152(2)		
O11-H11B···O2		107.0(8)						
O11-H11B···O7		165(2)			173(2)	162(2)		136(2)

the conclusion that Mn at M1 is trivalent. Based on geometric considerations, elongation of the O1-M1-O1 axis mainly influences the *a* cell dimension, whereas the variations in O5-M1-O5 distance affect both *b* and *c*.

Hydrogen bond systems in sursassite

The positions of H atoms and directions of the hydrogen bonds in sursassite are shown in Figure 6. All O-H bonds are located in mirror planes that are parallel to (010). This is also the situation in macfallite (Nagashima et al. 2008) and pumpellyite (Yoshiasa and Matsumoto 1985; Brigatti et al. 2006; Nagashima and Akasaka 2007). The relationships between donor and acceptor O atoms and their hydrogen bonds in sursassite can be summarized as follows: O6-H6A···O10 or O6-H6B···O3 and O6-H6B···O11, O7-H7···O11 or O7-H7···O2, O11-H11A···O2 and O11-H11A···O6 or O11-H11B···O2 and O11-H11B···O7. Two different H7 positions are shown in Figure 6 because H7 shows some lateral uncertainty, varying from structure to structure. The O2 atom only acts as an acceptor of H7 in the Molinello 1 sample. In general (for all other samples), O11 is an acceptor of the hydrogen bond from H7. Furthermore, there must be an additional partly occupied H site at O10 (H10) forming the hydrogen bond O10-H10···O6. However, the position of the proton at O10 could not be constrained in the present study. The H sites designated as A and B are approximately half-occupied. The H7 and H10 (not located) sites are postulated to be slightly more than half-occupied. This system of hydrogen bonds is in good agreement with the approximate H positions suggested by Mellini et al. (1984) for sursassite from Monte Alpe.

The best way to interpret the very complex hydrogen bonding system in sursassite is to use macfallite as a reference, because in macfallite the influence of disturbing divalent cations in M1 and M3 can be neglected (Fig. 7). Because of the absence of M^{2+} in M1 and the Jahn-Teller distortion due to Mn^{3+}, M1 octa-

TABLE 6. Refined site-scattering values* and assigned site occupancy† for the M1, M2, M3, Mn1, and Mn2 sites

Sample	Site	Site-scattering	Site occupancy (apfu)‡	Number of electrons§
Flotta, Switzerland	M1	16.35(5)	Mg0.33Al0.36Mn0.31	16.39
	M2	12.96(5)	Al1.00	13
	M3	14.42(5)	Al0.88Mn0.12	14.44
	Mn1	22.55(6)	Mn0.61Ca0.39	23.05
	Mn2	24.67(6)	Mn1.00	25
New Brunswick, Canada	M1	16.3(1)	Mg0.29Al0.41Mn0.30	16.31
	M2	12.8(1)	Al1.00	13
	M3	13.3(1)	Al1.00	13
	Mn1	23.1(1)	Mn0.78Ca0.22	23.50
	Mn2	24.4(1)	Mn1.00	25
Kamisugai, Japan	M1	18.7(1)	Mg0.31Al0.19Mn0.50	18.69
	M2	12.9(1)	Al1.00	13
	M3	14.0(1)	Al0.92Mn0.08	13.96
	Mn1	22.9(1)	Mn0.70Ca0.30	23.50
	Mn2	24.4(1)	Mn1.00	25
Kamogawa, Japan	M1	15.63(9)	Mg0.23Al0.54Mn0.18Fe0.05	15.58
	M2	12.88(9)	Al1.00	13
	M3	13.35(9)	Al0.97Mn0.03	13.36
	Mn1	23.04(9)	Mn0.66Ca0.34	23.30
	Mn2	24.7(1)	Mn1.00	25
Molinello, Italy (Specimen 1)	M1	13.79(8)	Mg0.26Al0.66Mn0.05Cu0.03	13.82
	M2	12.90(8)	Al1.00	13
	M3	13.71(8)	Al0.94Mn0.06	13.72
	Mn1	22.50(9)	Mn0.66Ca0.34	23.3
	Mn2	24.75(9)	Mn1.00	25
Molinello, Italy (Specimen 2)	M1	16.5(2)	Mg0.19Cu0.12Al0.53Mn0.16	16.65
	M2	12.7(2)	Al1.00	13
	M3	13.1(2)	Al1.00	13
	Mn1	22.9(2)	Mn0.61Ca0.39	23.05
	Mn2	23.8(3)	Mn1.00	25
Gambatesa, Italy	M1	14.2(1)	Mg0.28Al0.60Mn0.12	14.16
	M2	13.2(1)	Al1.00	13
	M3	13.8(1)	Al0.94Mn0.06	13.72
	Mn1	22.9(2)	Mn0.53Ca0.47	22.65
	Mn2	24.8(2)	Mn1.00	25

* The site-scattering values were determined from the site occupancies of manganese at Mn1 and Mn2 and aluminum at M1, M2, and M3, refined without any constraints.
† Elements with less than 0.05 apfu by EMPA analysis were neglected.
‡ Site occupancy is estimated from site-scattering and results of electron microprobe analyses.
§ Calculated from the site occupancy assuming neutral atoms.

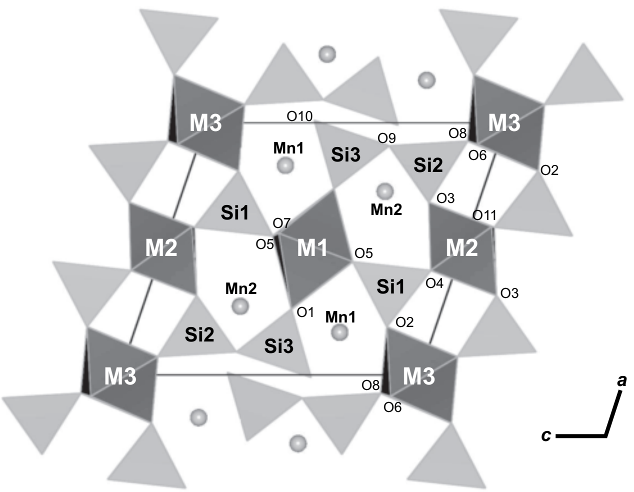

FIGURE 2. Crystal structure of sursassite projected parallel to [010] using the program VESTA (Momma and Izumi 2008).

hedral ligands in macfallite are not hydroxylated. In sursassite, significant M^{2+} content in M1 requires partial hydroxylation of M1 ligands. In this study, we located ca. 50% OH at O7 forming a hydrogen bond to O11. Thus, for occupied H7, a different proton position at O11 (compared to macfallite) is required. H11A avoids too close a distance to H7 and forms a hydrogen bond O11–H11A···O6 crossing the narrow **b**-channels surrounded by $M2O_6$, $Si2O_4$, $M3O_6$, and $Si1O_4$ polyhedra (Fig. 6). This situation leaves two possibilities: (1) the proton at O6 adjusts to the position H6A forming the hydrogen bond O6-H6A···O10, or (2) H6B and H11A, both close to each other within the narrow channels, are dynamically disordered as in lawsonite at room temperature (Libowitzky and Armbruster 1995; Libowitzky and Rossman 1996).

Of particular interest is the role of O10 bonded to Si3. We would expect H10, linked to O10, to form an OH group whenever H6A is vacant. The O10 atom acts as an acceptor for the strong hydrogen bond O6-H6A···O10 with an O6···O10 distance of about 2.66–2.67 Å. Ferraris and Ivaldi (1988) showed that for short O-H···O donor-acceptor distances, the acceptor benefits from an additional ca. 0.25 valence unit (v.u.) from the proton. The O10 site is associated with a bond-valence sum of 1.34–1.43 v.u. Although O10 benefits from an increase of 0.25 v.u. due to its strong acceptor role for H6A, the bond valence sum value remains too small, implying that O10 partially represents a silanol group. In addition, calculated chemical formulae of sursassite indicate more than 3 OH apfu, even with all Mn at M1 and M3 considered trivalent.

In macfallite, O10 represents a fully occupied silanol group with lengthened Si3-O10 bond (Nagashima et al. 2008), as predicted by Nyfeler and Armbruster (1998). This lengthening is not observed in sursassite. In contrast, the Si3-O10 bond is

Table 7. Calculated bond valences (v.u.) in sursassite

Cation/anion	Mn1	Mn2	M1	M2	M3	Si1	Si2	Si3	$ΣC^v$
Flotta, Switzerland									
O1	0.271†	0.275†	0.332†					1.011†	1.889
O2	0.356†				0.510†	1.056†			1.922
O3		0.387†		0.526†			1.076†		1.989
O4				0.488†‡		1.003			1.979
O5		0.132	0.430†‡			0.960			1.952
O6					0.568†‡				1.136
O7	0.346		0.556†‡						1.458
O8	0.221				0.396†‡		0.968		1.981
O9	0.198						0.968	0.925	2.091
O10		0.341						1.008	1.349
O11				0.540†					1.080
$ΣA^v$	2.019	1.797	2.636	3.108	2.948	4.075	4.088	3.955	
New Brunswick, Canada									
O1	0.265†	0.277†	0.343†					0.995†	1.880
O2	0.349†				0.514†	1.053†			1.916
O3		0.391†		0.522†			1.076†		1.989
O4				0.491†‡		0.989			1.971
O5		0.135	0.444†‡			0.984			2.007
O6					0.569†‡				1.138
O7	0.349		0.586†‡						1.521
O8	0.214				0.395†‡		0.947		1.951
O9	0.180						0.987	0.930	2.097
O10		0.340						1.050	1.390
O11				0.533†					1.066
$ΣA^v$	1.971	1.811	2.746	3.092	2.956	4.079	4.086	3.970	
Kamisugai, Japan									
O1	0.274†	0.280†	0.331†					1.008†	1.893
O2	0.350†				0.522†	1.058†			1.930
O3		0.383†		0.521†			1.082†		1.986
O4				0.490†‡		0.981			1.961
O5		0.153	0.448†‡			0.992			2.041
O6					0.572†‡				1.152
O7	0.360		0.608†‡						1.576
O8	0.214				0.393†‡		0.953		1.953
O9	0.186						0.965	0.940	2.091
O10		0.318						1.022	1.340
O11				0.539†					1.078
$ΣA^v$	2.008	1.797	2.774	3.100	2.974	4.089	4.082	3.978	
Kamogawa, Japan									
O1	0.271†	0.275†	0.337†					1.005†	1.888
O2	0.355†				0.517†	1.056†			1.928
O3		0.388†		0.528†			1.076†		1.972
O4				0.489†‡		0.997			1.975
O5		0.136	0.434†‡			0.963			1.967
O6					0.574†‡				1.148
O7	0.352		0.562†‡						1.476
O8	0.222				0.398†‡		0.965		1.983
O9	0.194						0.963	0.935	2.092
O10		0.332						1.041	1.373
O11				0.539†					1.078
$ΣA^v$	2.020	1.794	2.666	3.112	2.978	4.072	4.080	3.986	
Molinello, Italy (Specimen 1)									
O1	0.266†	0.271†	0.357†					0.987†	1.881
O2	0.361†				0.512†	1.050†			1.923
O3		0.391†		0.532†		.	1.082†		2.005
O4				0.490†‡		1.000			1.980
O5		0.117	0.434†‡			0.960			1.945
O6					0.582†‡				1.164
O7	0.335		0.548†‡						1.431
O8	0.229				0.405†‡		0.963		2.002
O9	0.196						0.965	0.937	2.098
O10		0.352						1.073	1.425
O11				0.535†					1.070
$ΣA^v$	2.014	1.793	2.678	3.114	2.998	4.060	4.092	3.984	
Molinello, Italy (Specimen 2)									
O1	0.276†	0.274†	0.337†					0.981†	1.868
O2	0.373†				0.501†	1.058†			1.932
O3		0.380†		0.510†		.	1.126†		2.016
O4				0.488†‡		0.984			1.960
O5		0.131	0.421†‡			1.003			1.976
O6					0.560†‡				1.120
O7	0.367		0.563†‡						1.493
O8	0.223				0.387†‡		0.989		1.986
O9	0.193						0.992	0.920	2.105
O10		0.319						1.090	1.409

Continued on next page

Table 7.—*CONTINUED*

Cation/anion	Mn1	Mn2	M1	M2	M3	Si1	Si2	Si3	ΣC^v
Molinello, Italy (Specimen 2)									
O11				0.537†					1.074
ΣA^v	2.081	1.758	2.642	3.070	2.896	4.103	4.233	3.972	
Gambatesa, Italy									
O1	0.281†	0.271†	0.348†					0.981†	1.881
O2	0.369†				0.512†	1.050†			1.931
O3		0.380†		0.535†		.	1.079†		1.942
O4				0.486†‡		0.987			1.959
O5		0.115	0.431†‡			0.984			1.964
O6					0.576†‡				1.152
O7	0.348		0.543†‡						1.434
O8	0.238				0.396†‡		0.987		2.017
O9	0.204						0.984	0.925	2.113
O10		0.335						1.058	1.393
O11				0.536†					1.072
ΣA^v	2.090	1.752	2.644	3.114	2.968	4.071	4.129	3.945	

Note: ΣA^v is the valence of bonds emanating from cations summed over the bonded anions. ΣC^v is the valence of bonds reaching anions.
† Two bonds per cation.
‡ Two bonds per anion.

the shortest one within the Si3 tetrahedron (Table 5). Thus, a complete silanol group at O10 in sursassite can be excluded. In addition, we were unable to locate a hydrogen site close to O10, although bond-valence sums and charge-balance requirements suggest its existence. We assume that the difference in the Si3-O10 bond lengths, depending on whether H10 is occupied (Nyfeler and Armbruster 1998), causes O10 disorder, making the detection of a partially occupied H10 site in difference-Fourier maps very difficult (impossible in our case).

The ATR-FTIR spectrum of sursassite in the region of OH-stretching vibrations is characterized by two OH bands at 3511 and 3262 cm^{-1}, and one additional broad band at 2950 cm^{-1}. The associated OH···O distances (Table 9) were calculated using the correlation between the observed OH-stretching band wavenumbers and the O···O distances in angstroms, as given by Libowitzky (1999). The two strongest OH bands result from relatively weak hydrogen bonds associated with the O7 and O11 sites, in agreement with the H positions determined in the structure refinement and analysis of the bond-valence sums. The band at 3511 cm^{-1} is assigned to O7···O11 and O11···O2, and the one at 3262 cm^{-1} to O11···O6 bonds. The broad band at ca. 2950 cm^{-1} is assigned to an OH-stretching vibration associated with the

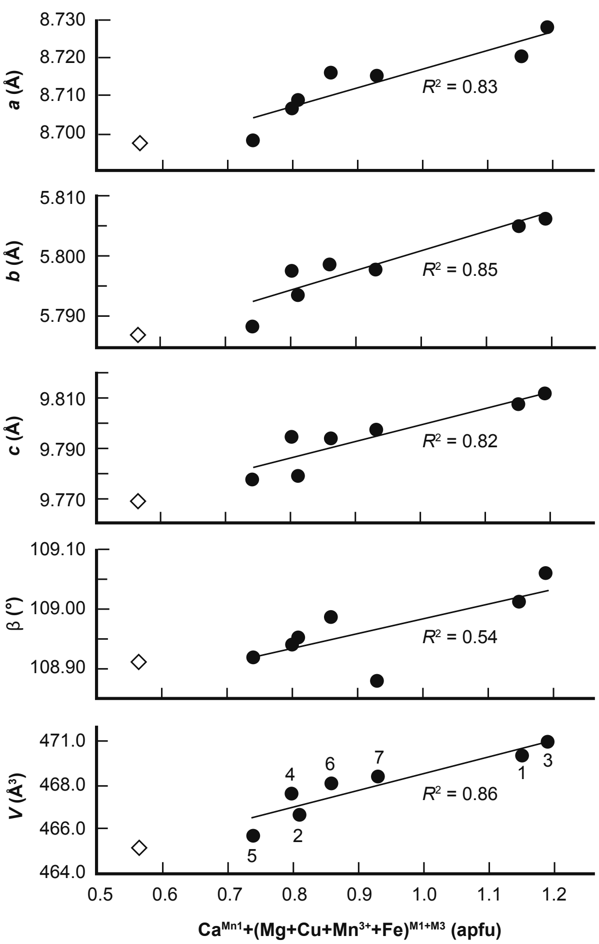

Figure 3. Variations of unit-cell parameters (Å) as a function of Ca^{Mn1}+(Mg+Cu+Mn+Fe)$^{M1+M3}$ (apfu); e.s.d. values of plotted values are considerably smaller than the symbol size. Closed circles denote sursassites in this study. Open diamond denotes sursassite data obtained by Hatert et al. (2008). Sample numbers are given in Tables 1 and 2.

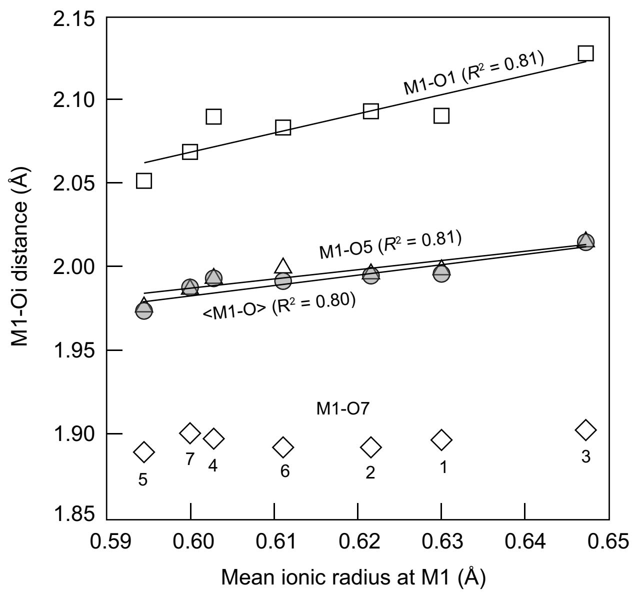

Figure 4. Variations of M1-Oi distance (Å) as a function of mean ionic radius at M1 (Å); e.s.d. values of plotted values are considerably smaller than the symbol size. Sample numbers are given in Tables 1 and 2.

TABLE 8. Bond-length* and angular† distortions for the octahedral sites

Sample	M1 site		M2 site		M3 site	
	DI	$\sigma_\theta(\mathrm{oct})^2$	*DI*	$\sigma_\theta(\mathrm{oct})^2$	*DI*	$\sigma_\theta(\mathrm{oct})^2$
Falotta, Switzerland	0.033	17.40	0.007	35.34	0.029	26.57
New Brunswick, Canada	0.033	17.64	0.006	34.40	0.028	27.85
Kamisugai, Japan	0.038	14.92	0.007	37.19	0.029	25.91
Kamogawa, Japan	0.032	16.88	0.008	35.15	0.028	28.27
Molinello, Italy (Specimen 1)	0.028	19.40	0.007	33.44	0.026	28.27
Molinello, Italy (Specimen 2)	0.034	17.47	0.007	36.56	0.028	25.65
Gambatesa, Italy	0.029	16.98	0.009	34.51	0.028	27.38

* Bond-length distortion parameter defined by Baur (1974); *DI* (oct) = $1/6\ \Sigma|R_i - R_{avg}|/R_{avg}$, where R_i is each bond length and R_{avg} is the average distance for an octahedron.

† Angular distortion parameter defined by Robinson et al. (1971); $\sigma_\theta(\mathrm{oct})^2 = \Sigma(\theta i - 90°)/11$ (θi: O-M-O angle).

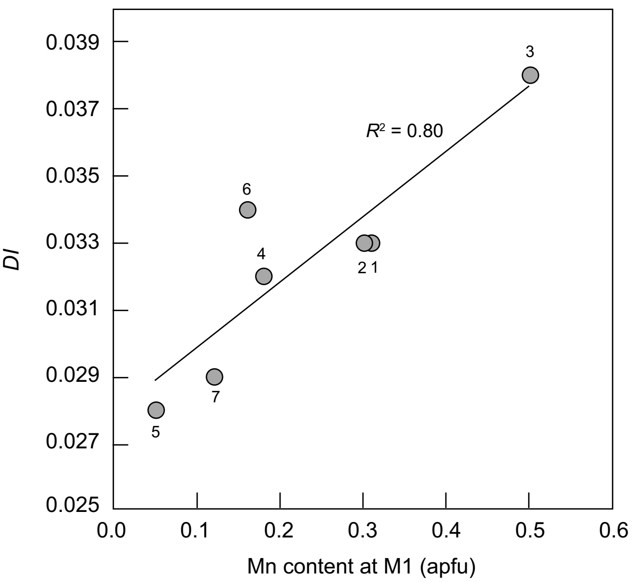

FIGURE 5. Relationship between the mean ionic radius of M1 site and bond-length distortion (*DI*) of $M1O_6$ octahedra. Definition is given in Table 8. Sample numbers are given in Tables 1 and 2.

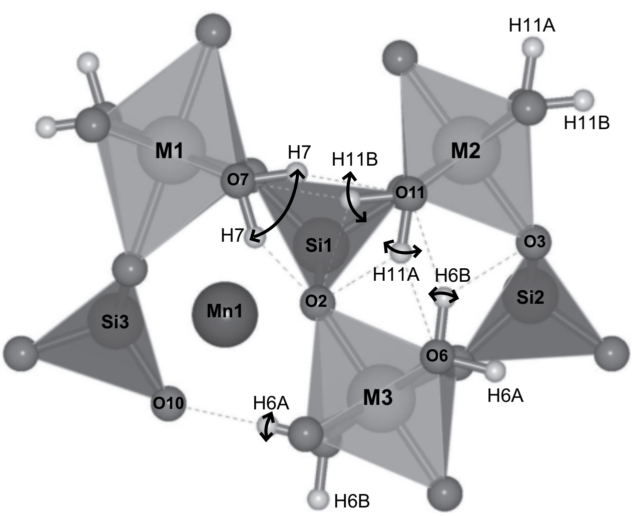

FIGURE 6. Hydrogen positions and hydrogen bonds in sursassite projected parallel to [010]. Dashed lines indicate H···O bonds. The arrows show the range of H positions.

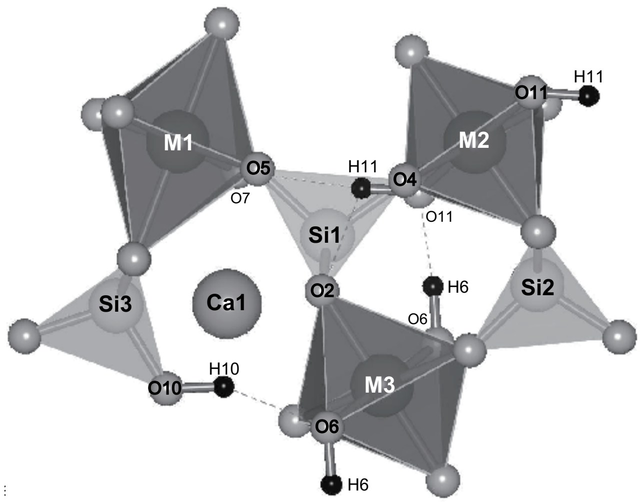

FIGURE 7. Hydrogen positions and hydrogen bonds in macfallite (Nagashima et al. 2008) projected parallel to [010]. Dashed lines indicate H···O bonds.

TABLE 9. Hydroxyl streching wavenumbers and corresponding O···O distances in sursassite from New Brunswick, Canada

OH-stretching wavenumber (cm^{-1})		*d* (O···O) (Å)
ATR	KBr pellet	
3511	3511	2.92
3262	3275	2.73
~2950	~2980	2.64

Note: Bond assignment according to Libowitzky (1999).

O6-H6···O10 or the O10-H10···O6 bond with an O···O separation of about 2.66–2.67 Å.

The infrared spectrum of macfallite also shows a broad band around 2900 cm^{-1} (Nagashima et al. 2008). In case of macfallite, this broad band was assigned to O6···O11 representing hydrogen bonds, which cross the narrow channel diagonally (Fig. 7). The O6···O11 distance (2.73–2.75 Å) of sursassite is substantially longer than that of macfallite (2.63 Å), thus requiring the different assignment.

Intergrowth of pumpellyite domains in sursassite

The sursassite structure is related to the pumpellyite structure by a shift of $(a + c)/2$ (Mellini et al. 1984). A high-resolution transmission-electron microscope study by Mellini et al. (1984) established the existence of pumpellyite-sursassite intergrowths. Diffraction data of some sursassite crystals investigated in this study also imply the existence of pumpellyite domains within

TABLE 10. Difference-Fourier peaks of sursassite

	x	y	z	Position in pumpellyite
Kamogawa,	0	0	1/2	X
Japan	0.337	3/4	0.502	Si3
	0.245	1/4	0.320	W2
	0.348	1/4	0.682	W1
Molinello,	0.348	1/4	0.685	W1
Italy	0.252	1/4	0.330	W2
(Specimen 1)	0	0	1/2	X
	0.338	3/4	0.504	Si3

sursassite. Difference-Fourier peaks of Kamogawa and Molinello 1 sursassite samples are listed in Table 10. These two samples show four relatively strong residual peaks in their difference-Fourier maps. Based on topological considerations, the peaks can be assigned to W1, W2, X, and Si3 of the pumpellyite structure. Such residual peaks are not observed for the Falotta sursassite indicating that the proportion of pumpellyite domains in sursassite varies from zero (Falotta) to 5% (Kamogawa and Molinello specimen 1).

ACKNOWLEDGMENTS

We thank A. Chakhmouradian, associate editor, F. Hatert, R. Peterson, and an anonymous referee for their constructive comments on this manuscript. This research was supported by Japan Society for the Promotion of Science (JSPS) for research abroad to M. Nagashima. One of the authors (M.A.) was supported by Grant-in-Aid for Scientific Research on Innovative Areas (no. 20103002) from the Ministry of Education, Culture, Sports, Science and Technology (MEXT) of Japan.

REFERENCES CITED

Albee, A. and Chodos, A.A. (1970) Semiquantitative electron microprobe determination of Fe^{2+}/Fe^{3+} and Mn^{2+}/Mn^{3+} in oxides and silicates and its application to petrologic problems. American Mineralogist, 55, 491–501.
Allmann, R. (1984) Die struktur des sursassits und ihre beziehung zur pumpellyit- und ardennitstruktur. Fortschritte der Mineralogie Beiheft, 62, 3–4 (in German).
Baur, H. (1974) The geometry of polyhedral distortions. Predictive relationships for the phosphate group. Acta Crystallographica, B30, 1195–1215.
Brese, N.E. and O'Keeffe, M. (1991) Bond-valence parameters for solids. Acta Crystallographica, B47, 192–197.
Brigatti, M.F., Caprilli, E., and Marchesini, M. (2006) Poppiite, the V^{3+} end-member of the pumpellyite group: Description and crystal structure. American Mineralogist, 91, 584–588.
Brown, I.D. and Altermatt, D. (1985) Bond-valence parameters obtained from a systematic analysis of the inorganic crystal structure database. Acta Crystallographica, B41, 244–247.
Bruker (1999) SMART and SAINT-Plus. Versions 6.01. Bruker AXS Inc., Madison, Wisconsin.
Cortesogno, L., Lucchetti, G., and Penco, A.M. (1979) Le mineralizzazioni a manganese nei diaspri delle ofioliti liguri: mineralogia e genesi. Rendiconti Società Italiana Mineralogia e Petrologia, 35, 151–197 (in Italian).
Ferraris, G. and Ivaldi, G. (1988) Bond valence *vs* bond length in O…O hydrogen bonds. Acta Crystallographica, B44, 341–344.
Ferraris, G., Mellini, M., and Merlino, S. (1986) Polysomatism and the classification of minerals. Rendiconti Societa Italiana Di Mineralogia e Petrologia, 44, 181–192.
Ferraris, G., Makovicky, E., and Merlino, S. (2004) 1.8 Merotype and plesiotype series, p. 57–110. Crystallography of Modular Materials, Oxford University Press, U.K.
Franks, F., Ed. (1973) Water: A Comprehensive Treatise, 2, 684 p. Plenum, New York.
Freed, R.L. (1964) An X-ray study of sursassite from New Brunswick. American Mineralogist, 49, 168–173.
Gottschalk, M., Fockenberg, T., Grevel, K.-D., Wunder, B., Wirth, R., Schreyer, W., and Maresch, W.V. (2000) Crystal structure of the high-pressure phase $Mg_4(MgAl)Al_4[Si_6O_{21}/(OH)_7]$: an analogue of sursassite. European Journal of Mineralogy, 12, 935–945.
Hatert, F., Fransolet, A.-M., Wouters, J., and Bernhardt, H.-J. (2008) The crystal structure of sursassite from the Lienne Valley, Stavelot Massif, Belgium. European Journal of Mineralogy, 20, 993–998.
Hawthorne, F.C., Ungaretti, L., and Oberti, R. (1995) Site populations in minerals: Terminology and presentation of results of crystal-structure refinement. Canadian Mineralogist, 33, 907–911.
Heinrich, E.W. (1962) Sursassite from New Brunswick. Canadian Mineralogist, 7, 291–300.
Jakob, J. (1926) Sursassite, ein mangansilikat aus dem Val d'Err (Graubünden). Schweizerische Mineralogische und Petrographische Mitteilungen, 6, 376–380 (in German).
——— (1931) Über die chemische formel und die optischen daten des sursassit. Schweizerische Mineralogische und Petrographische Mitteilungen, 11, 178–180 (in German).
——— (1933) Die Manganerzlagerstätten zwischen Val d'Err und Roffna (Oberhalbstein), ihre begleitminerale und ihre genesis. Schweizerische Mineralogische und Petrographische Mitteilungen, 13, 17–39 (in German).
Kimura, Y. and Akasaka, M. (1999) Estimation of Fe^{2+}/Fe^{3+} and Mn^{2+}/Mn^{3+} ratios by electron probe micro analyzer. Journal of the Mineralogical Society of Japan, 28, 159–166 (in Japanese with English abstract).
Libowitzky, E. (1999) Correlation of O-H stretching frequencies and O-H···O hydrogen bond lengths in minerals. Monatshefte für Chemie, 130, 1047–1059.
Libowitzky, E. and Armbruster, T. (1995) Low-temperature phase transitions and the role of hydrogen bonds in lawsonite. American Mineralogist, 80, 1277–1285.
Libowitzky, E. and Rossman, G.R. (1996) FTIR spectroscopy of lawsonite between 82 and 325 K. American Mineralogist, 81, 1080–1091.
Marchesini, M. and Pagano, R. (2001) The Val Graveglia manganese district, Liguria, Italy. The Mineralogical Record, 32, 349–379; 415.
Mellini, M., Merlino, S., and Pasero, M. (1984) X-ray and HRTEM study of sursassite: Crystal structure, stacking disorder, and sursassite-pumpellyite intergrowth. Physics and Chemistry of Minerals, 10, 99–105.
Minakawa, T. (1992) Study on characteristic mineral assemblages and formation process of metamorphosed manganese ore deposits in the Sanbagawa belt. Memoirs of the Faculty of Science, Ehime University, 1, 1–74 (Japanese with English abstract).
Minakawa, T. and Momoi, H. (1987) Occurrences of ardennite and sursassite from the metamorphic manganese deposits in the Sanbagawa belt, Shikoku, Japan. Journal of the Mineralogical Society of Japan, 18, 87–98 (Japanese with English abstract).
Momma, K. and Izumi, F. (2008) VESTA: a three-dimensional visualization system for electronic and structural analysis. Journal of Applied Crystallography, 41, 653–658.
Moore, P.B., Shen, J., and Araki, T. (1985) Crystal chemistry of the $^{2}_{\infty}[M_2^{3+}\phi_2(TO_4)_2]$ sheet: Structural principles and crystal structures of ruizite, macfallite and orientite. American Mineralogist, 70, 171–181.
Nagashima, M. and Akasaka, M. (2007) The distribution of chromium in chromian pumpellyite from Sarani Urals, Russia: A TOF neutron and X-ray Rietveld study. Canadian Mineralogist, 45, 837–846.
Nagashima, M., Rahmoun, N.-S., Alekseev, E.V., Geiger, C.A., Armbruster, T., and Akasaka, M. (2008) Crystal chemistry of macfallite: Relationships to sursassite and pumpellyite. American Mineralogist, 93, 1851–1857.
Nyfeler, D. and Armbruster, T. (1998) Silanol groups in minerals and inorganic compounds. American Mineralogist, 83, 119–125.
Reddy, B.J. and Frost, R.L. (2007) Electronic and vibrational spectra of Mn rich sursassite. Spectrochimica Acta Part A, 66, 312–317.
Reinecke, T. (1986) Phase relationships of sursassite and other Mn-silicates in highly oxidized low-grade, high-pressure metamorphic rocks from Evvia and Andros Islands, Greece. Contributions to Mineralogy and Petrology, 94, 110–126.
Robinson, K., Gibbs, G.V., and Ribbe, P.H. (1971) Quadratic elongation: A quantitative measure of distortion in coordination polyhedra. Science, 172, 567–570.
Sheldrick, G.M. (1996) SADABS. University of Göttingen, Germany.
——— (1997) SHELXL-97. A program for crystal structure refinement. University of Göttingen, Germany.
——— (2002) TWINABS. Bruker-AXS, Madison, Wisconsin.
Yoshiasa, A. and Matsumoto, T. (1985) Crystal structure refinement and crystal chemistry of pumpellyite. American Mineralogist, 70, 1011–1019.

MANUSCRIPT RECEIVED FEBRUARY 20, 2009
MANUSCRIPT ACCEPTED JUNE 8, 2009
MANUSCRIPT HANDLED BY ANTON CHAKHMOURADIAN

TABLE 3 Refined atomic positions of sursassite

Site	neq*	W†		Flotta, Switzerland	New Brunswick, Canada	Kamisugai, Japan	Kamogawa, Japan	Molinello, Italy (Specimen 1)	Molinello, Italy (Specimen 2)	Gambatesa, Italy
Mn1	2	*e*	*x*	0.16884(5)	0.1700(1)	0.1706(1)	0.16902(8)	0.16738(8)	0.1699(3)	0.1677(2)
			y	1/4	1/4	1/4	1/4	1/4	1/4	1/4
			z	0.31355(4)	0.3131(1)	0.31322(9)	0.31367(7)	0.31398(7)	0.3132(2)	0.3142(1)
Mn2	2	*e*	*x*	0.27223(5)	0.2717(1)	0.2763(1)	0.27275(9)	0.26707(9)	0.2716(3)	0.2693(2)
			y	1/4	1/4	1/4	1/4	1/4	1/4	1/4
			z	0.67531(4)	0.6748(1)	0.67528(9)	0.67567(7)	0.67527(6)	0.6753(2)	0.6760(1)
Si1	2	*e*	*x*	0.30787(7)	0.3072(2)	0.3071(2)	0.3071(1)	0.3078(1)	0.3072(4)	0.3074(2)
			y	3/4	3/4	3/4	3/4	3/4	3/4	3/4
			z	0.19109(6)	0.1917(2)	0.1906(1)	0.1913(1)	0.1925(1)	0.1919(4)	0.1923(2)
Si2	2	*e*	*x*	0.20691(7)	0.2065(2)	0.2071(2)	0.2067(1)	0.2069(1)	0.2064(4)	0.2066(2)
			y	3/4	3/4	3/4	3/4	3/4	3/4	3/4
			z	0.80740(6)	0.8067(2)	0.8072(1)	0.8080(1)	0.8078(1)	0.8076(4)	0.8077(2)
Si3	2	*e*	*x*	0.15557(7)	0.1545(2)	0.1532(2)	0.1554(1)	0.1573(1)	0.1545(4)	0.1566(2)
			y	3/4	3/4	3/4	3/4	3/4	3/4	3/4
			z	0.49480(6)	0.4941(2)	0.4952(2)	0.4950(1)	0.4944(1)	0.4945(4)	0.4947(2)
M1	2	*d*	*x*	1/2	1/2	1/2	1/2	1/2	1/2	1/2
			y	0	0	0	0	0	0	0
			z	1/2	1/2	1/2	1/2	1/2	1/2	1/2
M2	2	*b*	*x*	1/2	1/2	1/2	1/2	1/2	1/2	1/2
			y	0	0	0	0	0	0	0
			z	0	0	0	0	0	0	0
M3	2	*a*	*x*	0	0	0	0	0	0	0
			y	1/2	1/2	1/2	1/2	1/2	1/2	1/2
			z	0	0	0	0	0	0	0
O1	4	*f*	*x*	0.2608(1)	0.2601(3)	0.2566(3)	0.2607(2)	0.2654(2)	0.2617(7)	0.2638(4)
			y	0.5139(2)	0.5132(5)	0.5130(5)	0.5138(4)	0.5140(4)	0.514(1)	0.5135(6)
			z	0.5013(1)	0.5005(3)	0.5004(3)	0.5017(2)	0.5027(2)	0.5015(6)	0.5027(4)
O2	4	*f*	*x*	0.1916(1)	0.1907(3)	0.1908(3)	0.1907(2)	0.1916(2)	0.1912(6)	0.1912(4)
			y	0.5248(2)	0.5246(5)	0.5258(5)	0.5248(3)	0.5238(3)	0.525(1)	0.5245(6)
			z	0.1631(1)	0.1630(3)	0.1628(3)	0.1628(2)	0.1637(2)	0.1639(6)	0.1631(4)
O3	4	*f*	*x*	0.3146(1)	0.3142(3)	0.3151(3)	0.3145(2)	0.3143(2)	0.3134(7)	0.3146(4)
			y	0.5180(2)	0.5177(5)	0.5191(5)	0.5180(3)	0.5174(3)	0.521(1)	0.5184(6)
			z	0.8332(1)	0.8332(3)	0.8328(3)	0.8339(2)	0.8342(2)	0.8328(6)	0.8353(4)
O4	2	*e*	*x*	0.4148(2)	0.4141(5)	0.4142(5)	0.4152(3)	0.4154(3)	0.414(1)	0.4161(6)
			y	3/4	3/4	3/4	3/4	3/4	3/4	3/4
			z	0.0810(2)	0.0807(4)	0.0800(4)	0.0820(3)	0.0823(3)	0.0805(9)	0.0829(5)
O5	2	*e*	*x*	0.4491(2)	0.4487(5)	0.4492(5)	0.4484(3)	0.4482(3)	0.448(1)	0.4459(6)
			y	3/4	3/4	3/4	3/4	3/4	3/4	3/4
			z	0.3517(2)	0.3515(4)	0.3492(4)	0.3521(3)	0.3542(3)	0.351(1)	0.3532(5)
O6	2	*e*	*x*	0.0844(2)	0.0848(5)	0.0841(5)	0.0843(3)	0.0848(3)	0.085(1)	0.0845(6)
			y	1/4	1/4	1/4	1/4	1/4	1/4	1/4
			z	0.9289(2)	0.9294(4)	0.9283(4)	0.9291(3)	0.9295(3)	0.9288(9)	0.9291(5)
O7	2	*e*	*x*	0.4379(2)	0.4373(5)	0.4373(5)	0.4381(3)	0.4390(3)	0.438(1)	0.4391(7)
			y	1/4	1/4	1/4	1/4	1/4	1/4	1/4
			z	0.3690(2)	0.3690(4)	0.3682(4)	0.3684(3)	0.3692(3)	0.3695(9)	0.3679(5)
O8	2	*e*	*x*	0.0718(2)	0.0714(5)	0.0726(5)	0.0720(3)	0.0717(3)	0.0732(9)	0.0719(6)
			y	3/4	3/4	3/4	3/4	3/4	3/4	3/4
			z	0.8926(2)	0.8935(4)	0.8938(4)	0.8943(3)	0.8940(3)	0.8939(9)	0.8934(5)
O9	2	*e*	*x*	0.0902(2)	0.0893(5)	0.0886(5)	0.0899(3)	0.0912(3)	0.0901(9)	0.0921(6)
			y	3/4	3/4	3/4	3/4	3/4	3/4	3/4
			z	0.6360(2)	0.6366(4)	0.6369(4)	0.6370(3)	0.6363(3)	0.6376(9)	0.6375(5)
O10	2	*e*	*x*	-0.0103(2)	-0.0112(5)	-0.0131(5)	-0.0107(3)	-0.0074(4)	-0.008(1)	-0.0078(7)
			y	3/4	3/4	3/4	3/4	3/4	3/4	3/4
			z	0.3573(2)	0.3565(4)	0.3569(4)	0.3575(3)	0.3574(3)	0.3568(9)	0.3571(5)
O11	2	*e*	*x*	0.4114(2)	0.4121(5)	0.4106(5)	0.4119(3)	0.4129(3)	0.413(1)	0.4130(6)
			y	1/4	1/4	1/4	1/4	1/4	1/4	1/4
			z	0.0713(2)	0.0728(4)	0.0696(4)	0.0717(3)	0.0738(3)	0.0723(9)	0.0731(5)
H6A	2	*e*	*x*	0.05(1)	0.06(1)		0.06(1)	0.05(2)		
			y	1/4	1/4		1/4	1/4		
			z	0.8235(8)	0.824(1)		0.824(2)	0.824(1)		
H6B	2	*e*	*x*	0.203(1)			0.199(4)	0.201(3)		
			y	1/4			1/4	1/4		
			z	0.952(9)			0.94(1)	0.94(1)		
H7	2	*e*	*x*	0.454(9)	0.44(1)		0.44(1)	0.325(4)		0.45(3)
			y	1/4	1/4		1/4	1/4		1/4
			z	0.275(4)	0.269(3)		0.268(4)	0.31(1)		0.27(1)
H11A	2	*e*	*x*	0.294(2)	0.2932(7)		0.297(4)	0.295(2)		
			y	1/4	1/4		1/4	1/4		
			z	0.052(9)	0.034(8)		0.06(1)	0.05(1)		
H11B	2	*e*	*x*	0.40(1)			0.43(2)	0.40(1)		0.48(2)
			y	1/4			1/4	1/4		1/4
			z	0.168(4)			0.176(3)	0.168(6)		0.176(6)

* Multiplicity

† Wyckoff letter